PROCEEDINGS, 49th Workshop on Geothermal Reservoir Engineering
Stanford University, Stanford, California, February 12-14, 2024
SGP-TR-227

Using Petroleum Industry Data to Locate, Characterize, and Simulate a Hot Sedimentary Aquifer Geothermal Prospect

Alfred Lacazette[1], Stephen P. Cumella[2], Veit J. Matt[1], Mark G. Cottrell[3],
Saman Karimi[1,4], Bruce D. Marsh[1,4], William R. Chmela[1]

[1]Geothermal Technologies, Inc.; [2]C[2] Consulting; [3]WSP UK Ltd.; [4]Johns Hopkins University,
GTI mail: 108 Glenmore Ct., Bel Air, Maryland, 21014 USA
Corresponding author: alacazette@geothermal.tech

Keywords: geothermal, hot, sedimentary, aquifer, exploration, reservoir, characterization, simulation, Lyons, sandstone, Colorado

ABSTRACT

Hot sedimentary aquifer (HSA) geothermal exploits thick, porous, permeable aquifers for electricity generation, district heating, and direct-use applications. HSA temperatures are typically lower than traditional (hydrothermal) geothermal plays because high temperature over geologic time tends to destroy porosity by cementation. However, HSAs have substantial economic advantages over other geothermal resources. These advantages include long well life, large volumes of water, stable production temperature because water flow through the rock matrix more completely extracts the rock's heat, and typically there is no need to for expensive stimulation. In contrast, geothermal wells relying on flow in natural or induced fractures in impermeable rock can experience comparatively rapid cool-down because of the low thermal conductivity of rock and may require stimulation to promote sufficient fluid flow. Closed-loop systems have limited potential due to the low thermal conductivity of rock.

Existing oil and gas fields are good places to exploit HSAs in part because they are often hotter than surrounding areas (that's why the oil and gas are there) but especially because abundant, high-quality data has been collected by oil and gas operators. Such data includes log, core, seismic reflection, fluid, and pressure data. This presentation discusses the identification, characterization, and reservoir simulation of an HSA geothermal prospect in the Denver-Julesburg (DJ) Basin of Colorado using such existing data sets. The pilot, production, and injection well permits for this project are the first deep geothermal well permits ever granted by the state of Colorado.

The project targets the Permian age Lyons Fm., an eolian sandstone that averages ~40m thick in the area of interest. On the east side of the DJ Basin, the Lyons was deposited in a sabkha environment so that rock was completely cemented with anhydrite shortly after deposition. The anhydrite cement preserved the porosity through a long history of burial and diagenesis. Another diagenetic product was quartz cementation at quartz grain contacts. Subsequent fluid flow from the recharge area along the mountain front on the west to the discharge area in western Kansas removed the cement over large areas of the formation resulting in a strong, porous, and permeable rock. Density-porosity logs and core plug measurements show that the average porosity in the target area is 16%-17%, which is excellent. The horizontal and vertical permeabilities were determined from 71 core plug measurements and average 190-240 mD and 30-60 mD, respectively and a porosity-permeability transform was developed from these data. Elastic moduli, compressive strength, and sanding potential were determined from core testing. A few small, gentle anticlines in areas of porous Lyons trapped oil during regional fluid flow, but the formation is generally wet.

Thermal mapping utilized 6,181 corrected bottom hole temperatures from oil/gas wells. The correction procedure was validated with cased-hole temperature logs and a one-dimensional thermal model. Temperature, porosity, the depth to the potentiometric surface, and other quantities were mapped to identify suitable drilling targets. The maps were used to identify a target area with an expected temperature of 130°C. There is little structure in the area resulting in minimal formation dips. Pressure data and literature on DJ Basin hydrodynamics indicate that little or no natural flow is currently occurring in this underpressured reservoir. Fluid samples from a nearby oilfield were evaluated for corrosion and scaling potential.

A detailed static reservoir model of the prospect was built from representative well logs. The model included porosity, permeability, rock mechanics data, and other information. A producer-injector horizontal well pair was modeled with different well separations to determine the optimum spacing. Reservoir simulations with the FracMan™ software suite combined discrete fracture network and continuum methods into a hybrid model that captures the complexities of fluid-flow and temperature evolution in the complexly layered eolian sandstone. Pressure, temperature, fluid velocity, and fluid movement were tracked in three dimensions through time. Results show that the temperature of the produced water remains stable for over 20 years at a simultaneous production and injection rate of 100 kg/s. The detailed model was compared to a simple, homogeneous model run in the COMSOL™ software package. The results were similar, likely due to the high porosity and permeability of the rock. Pressure and temperature driven thermoelastic fracturing around the injector was estimated and mapped. Evaluation of sanding risk at the producing well is in progress as of this writing.

1. INTRODUCTION

Unlike wind and solar electricity generation, geothermal power is baseload and dispatchable, so that geothermal electricity does not require expensive energy storage systems and extensive, expensive systems of power lines and interconnections. Geothermal plants have a much smaller footprint than wind farms or solar gardens and require less material than wind or solar generation so that they have a substantially lower environmental impact than competing renewable resources. A geothermal power plant drops into the existing electric grid like a fossil fuel or nuclear power plant. Widespread implementation of geothermal electricity generation would therefore reduce the costs and environmental impacts of renewable energy systems and stabilize the electrical grid.

Almost all geothermally generated electricity is currently produced from hydrothermal systems of different types, often related to volcanism. Such systems are typically high temperature (>150 °C) and occur in naturally fractured rock with little to no matrix porosity and permeability. Hydrothermal power plants are clearly economical. The first hydrothermal power plant was built in 1904 in Tuscany, Italy, and hydrothermal plants around world are currently generating electricity. However, near-surface hydrothermal systems suitable for power generation are found over only a small fraction of the Earth's land surface (2-3%). Sedimentary basins cover a much larger fraction of the Earth's land surface and offshore on continental shelves. Consequently, exploiting Hot Sedimentary Aquifers (HSAs) could greatly increase both the amount and geographic coverage of geothermal electricity production. Recent technological advances in Organic Rankine Cycle (ORC) generating systems allow electricity generation from lower temperature HSAs, such as the Lyons Fm. Closed-loop geothermal systems have limited potential due to the low thermal conductivity of rock (White et al, 2024).

This paper describes such an HSA in the Denver-Julesburg (DJ) Basin. Figure 1 provides a location map of the study area, which is the "hot spot" of the prolific Wattenberg oil and gas field. Figure 2 is a schematic cross-section of the DJ Basin. The Paleozoic section, which includes the Permian-age Lyons Sandstone, is underpressured (Nelson et al, 2015). The Cretaceous shales form an aquiclude that isolates the underpressured interval from the overlying, overpressured, late Cretaceous age Niobrara and Codell Fms, which are the most important oil and gas producers in the basin (Figure 2). Fluid flow in the Lyons is from west to east with recharge along the mountain front and discharge into western Kansas (Lee and Bethke, 1994; Nelson et al, 2015). Pressure measurements in an oilfield in the study area and near our prospect show that the potentiometric surface of the Lyons is about 850m above sea level, which is equivalent to typical elevations in western Kansas. Consequently, we infer that little to no fluid flow is presently occurring.

This study relies exclusively on abundant data collected by the oil and gas industry. Our prospect is beneath active oil and gas production in the Niobrara Fm. This study shows why oil and gas fields are good places to exploit HSAs:

- The "hot spot" in the Wattenberg Field is both the warmest and most productive area of the field because the high geothermal gradients matured the hydrocarbon source rocks. In general, oil and gas fields tend to be hot and thus are good places to explore for geothermal resources.
- Because of the extensive oil and gas work, abundant log, core, 3D seismic, gravity, magnetic, and other essential data are readily available. Such rich data sets are unavailable for typical hydrothermal exploration programs.

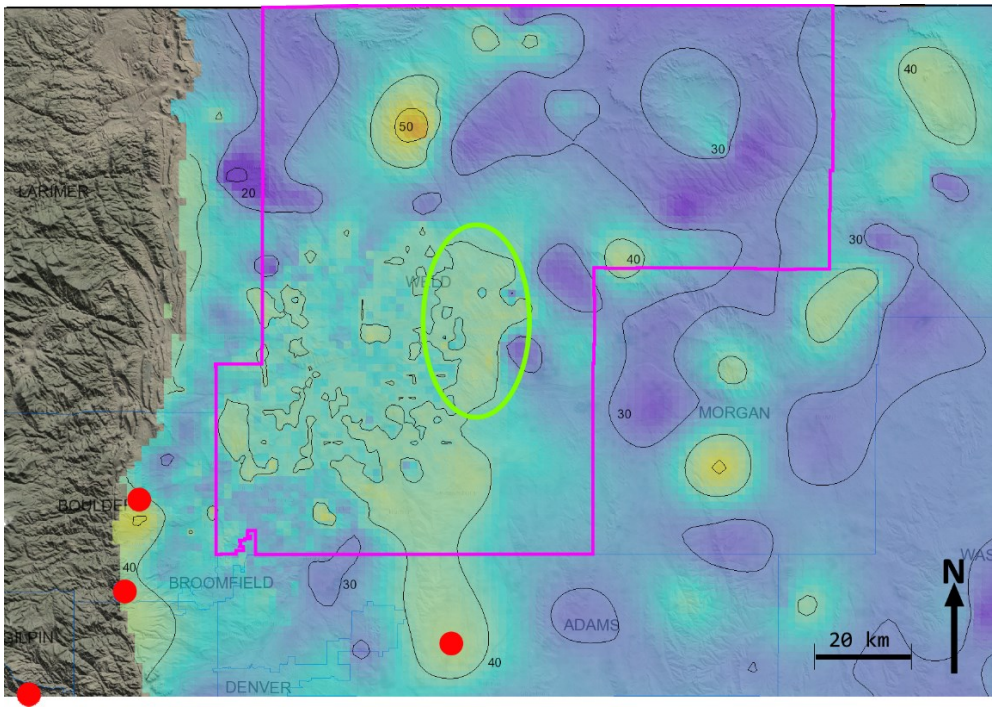

Figure 1: Location map of the study area after Colorado Geological Survey interactive online GIS map. Magenta outline: Weld County, Colorado, U.S.A. Green oval: Indicates the Wattenberg hot spot. Shading and contours east of the mountain front: Geothermal gradient between the Cretaceous age Mancos and Dakota Fms. Red dots: Hot springs.

2. GEOLOGY OF THE LYONS FM.

The Lyons Sandstone is an important source of building stone where it crops out on the western edge of the DJ Basin. To the east, the Lyons hosts eight oilfields in small anticlines associated with strike-slip faults. A comprehensive review of the stratigraphy and sedimentology of, and literature about, the Lyons Sandstone is provided by Kendigelen et al (2023). In a key paper, Levandowski et al (1973) describe the cementation and secondary porosity development of the Lyons. Lee and Bethke (1994) describe the diagenesis of the gray facies of the Lyons, which is associated with petroleum deposits. Nelson et al (2015) describe the hydrogeology of the Paleozoic section of the DJ Basin.

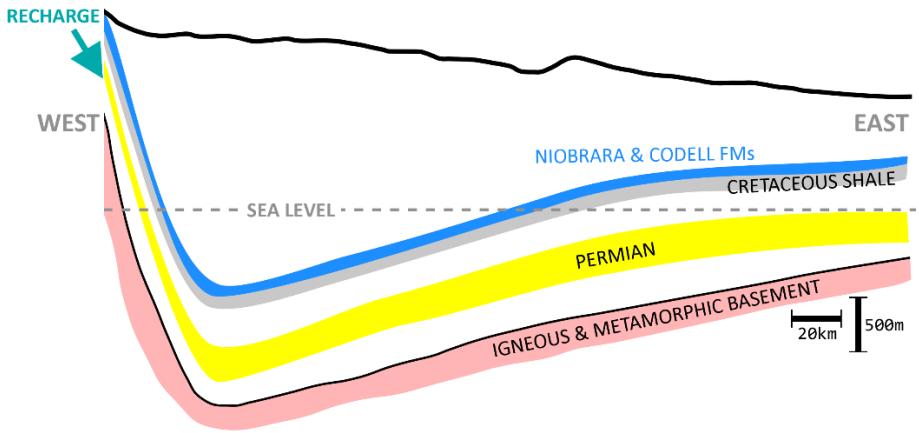

Figure 2: Schematic cross-section of the Denver-Julesburg (DJ) Basin. The Cretaceous shale is an aquiclude that isolates the underpressured Paleozoic section from the overpressured Niobrara and Codell Fms, which are the primary oil and gas producers. The Lyons Fm. is Permian age. Meteoric water enters the Paleozoic section along the mountain front and discharges eastwards into western Kansas.

2.1 Deposition

In the study area, the Lyons represents the oceanward edge of a Permian erg (an arid eolian sand sea). Kendigelen et al (2023) identify two depositional facies associations: 1) a dune-dominated facies comprising dunes and dry interdunes and 2) an interdune facies with damp to wet interdune deposits and ponds. They identify lateral changes in the interfingering facies associations with damp deposition dominating to the north and dryer conditions to the south. The changes in and distribution of these packages may be related to fluctuations in the groundwater table, changes in sediment supply, or other reasons.

The Lyons is tightly sealed above and below. The top seal is the Blaine Anhydrite. The bottom seal is the shales of the Satanka Fm.

2.2 Cementation and Cement Dissolution

In the study area, the Lyons was completely cemented with anhydrite and some calcite shortly after deposition (Levandowski et al, 1973). A proprietary study commissioned by GTI (Geothermal Technologies, Inc.) updated the earlier work with log and core data from more recently drilled wells (Longman, 2021). The study confirmed the earlier results but indicated that the permeability fairway is larger than indicated by Levandowski et al (1973). Early anhydrite cementation prevented the rock from being compacted during subsequent burial and lithification thereby preserving the original dune-sand porosity. Figure 3 clearly shows how the anhydrite and calcite cements overgrow the sand grains resulting in the preservation of primary porosity.

Pressure-solution resulted in quartz cementation at the quartz grain contacts. Later, fluid flow dissolved and removed much of the anhydrite cement in some areas of the Lyons Fm. and produced minor quartz overgrowths. The anhydrite cement removal and minor quartz cementation produced a rock with a strong skeleton and good porosity and permeability.

2.3 Porosity and Permeability

Horizontal and vertical porosity-permeability transforms were developed from 62 horizontal and 9 vertical core plugs from a well in a Lyons oilfield near our prospect (Figure 4).

Note that Zhou (2016) determined a porosity-permeability transform for the Lyons to evaluate geothermal well configurations. However, the samples used in that study had substantial bitumen and hence poorer porosity and permeability than core in the heart of our study area which is bitumen free. Hence, we did not include the data of Zhou (2016) in our porosity-permeability evaluation.

Density-porosity logs match the core porosity measurements well. Permeability logs were computed from the density-porosity logs using the transforms given in Figure 4. The logs were used for both mapping and for building a detailed static model for reservoir simulation.

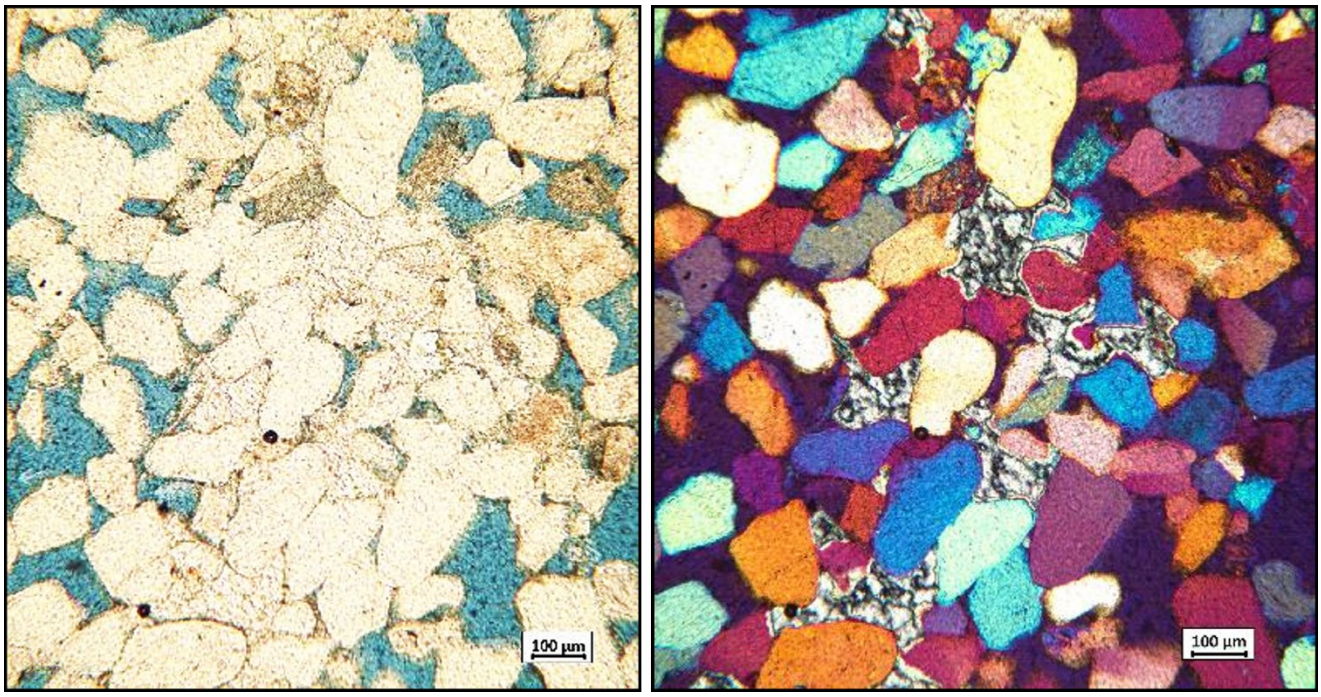

Figure 3: Thin section photomicrographs under plane light (LEFT) and crossed polars (RIGHT). Blue epoxy fills the pore space. These photos show a remnant patch of poikilotopic anhydrite cement (center, both photos) surrounded by loosely packed quartz sand grains with excellent intergranular porosity. Core analysis: Porosity 23.9%, permeability 253 mD. It is late-stage dissolution of the anhydrite that gives this sample its excellent reservoir quality (Longman, 2021).

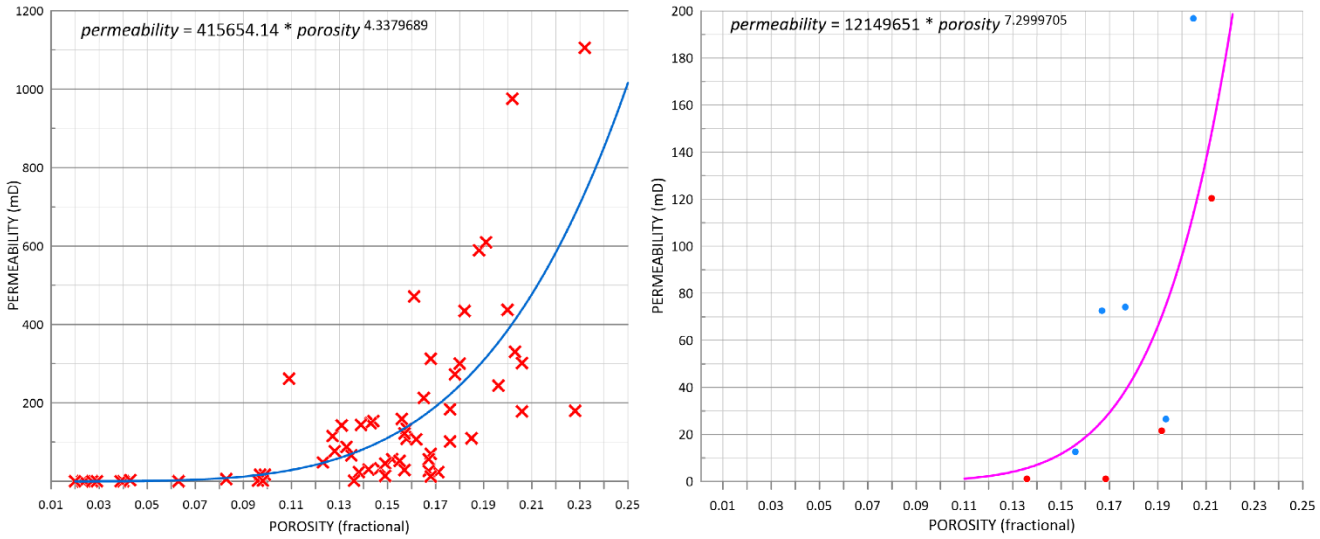

Figure 4: Horizontal (LEFT) and vertical (RIGHT) porosity-permeability transforms from core plug analyses.

3. EXPLORATION

Maps of the Lyons temperature, phi*h, flow-capacity (Kh*h), heat content, structure, and potentiometric surface depth were the basis of our exploration program. Mapping was accomplished with the Surfer™ software package. The mapping procedures utilized grid math in which the values at the nodes of the grids underlying the maps were used as variables to compute new quantities. For example, multiplying the map grid of the geothermal gradient by the map grid of the depth to the top of the Lyons results in a map grid of the

temperature at the top of the Lyons. All maps have the same grid geometry, which is square with a 250 m node spacing. Contouring of the maps was accomplished by Kriging.

3.1 Geothermal gradients and temperatures

We obtained 6,181 measurements of bottom-hole temperatures from oil/gas wells from various formations covering the Wattenberg "hot spot". The measurements were corrected for mud cooling using the correction of Corrigan and Bergman (1996) and Corrigan (2003). The correction was validated against cased-hole temperature logs and a one-dimensional thermal model derived from log data (Figure 5). Cased hole temperature logs are typically collected long after drilling and accurately reflect the undisturbed formation temperatures. Note that most bottom-hole temperature measurements were made at or above the Dakota so that the computed geothermal gradients may slightly overestimate the temperature at the Lyons.

The 1D basin model was constructed based on depth stratigraphic and lithologic data and calibrated to measured thermal and rock property data from interpreted geophysical well logs. The depth, stratigraphy (formation tops and ages), and lithologic data were used to reconstruct the burial history (deposition/erosion) as a function of the compaction behavior of the different lithologies by calibrating the model to measured rock bulk densities and porosities. The temperature data were used to calibrate the model to present-day thermal conditions by adjusting the present-day basal heat flow. For oil and gas work, such models can be calibrated to measured organic matter maturity (e.g. vitrinite reflectance), to estimate the thermal history. For geothermal exploration, paleo-conditions are of minor importance. They may help to understand the processes that have led to the present day geologic configuration, but are not essential to evaluate the present day geothermal potential of a prospect. In this study area, thermal maturity indicators do not coincide well with present-day temperatures.

Correctly constructed and calibrated 1D "Basin Models", utilizing all available geological and geophysical data, help to verify and QC measured data and support the estimation of critical thermal rock and fluid parameters (porosity, permeability, temperature, thermal conductivity, heat capacity, etc.) in areas and at depths where no direct measurements are available or obtainable.

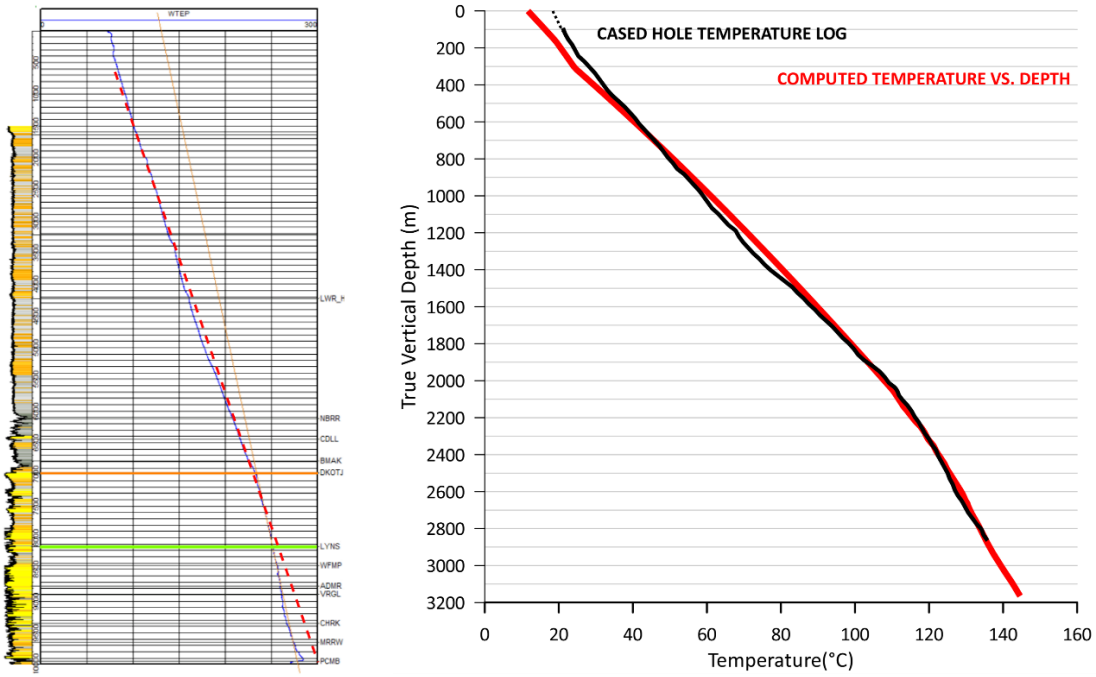

Figure 5: Cased hole temperature log from an oilfield and a one-dimensional thermal model used to validate the temperature correction. LEFT – Temperatures in °F, depths in ft. Blue line-cased hole temperature log. Yellow line – trend of the deep section. Dashed red line – trend of the shallow section. Green line – Lyons top. Orange line – Dakota top. RIGHT – Comparison between a cased-hole temperature log and a one-dimensional thermal model.

Geothermal gradients were then computed and mapped from the measurement depth and temperature (Figure 6). Most of the bullseyes on the map are supported by more than one measurement. Figure 6, right is a map of the temperature at the top of the Lyons calculated by multiplying the geothermal map grid by a map grid of the depth to the top of the Lyons from well log data. The depth map was made from measurements of the top of the Lyons, the top of the Codell, and a Codell-Lyons isopach map.

3.2 Mapping rock properties

Data on the depth, thickness, and other properties of the Lyons were obtained from both public and proprietary records. The data included logs, core, temperature, pressure, and other data typically collected in oilfields. The 3D seismic data was not available for this study, so the following results rely on exclusively on well data.

Density-porosity logs of the Lyons match the core plug data. The logs were used to compute phi*h and flow-capacity (Kh*h) and map these values. The resulting maps are shown in Figure 7.

Phi*h is the porosity-thickness and is computed by multiplying each log porosity value by the log sampling interval then summing the values for the entire formation. The result is in length units since porosity is dimensionless. If we think of a brine-filled rock, then the result is the depth of brine that would result if the rock was compacted to eliminate all the porosity (Figure 7, left). Also, phi*h can be computed for the *effective porosity*. The effective porosity sums only porosity ≥10%, which is the porosity with the best permeability.

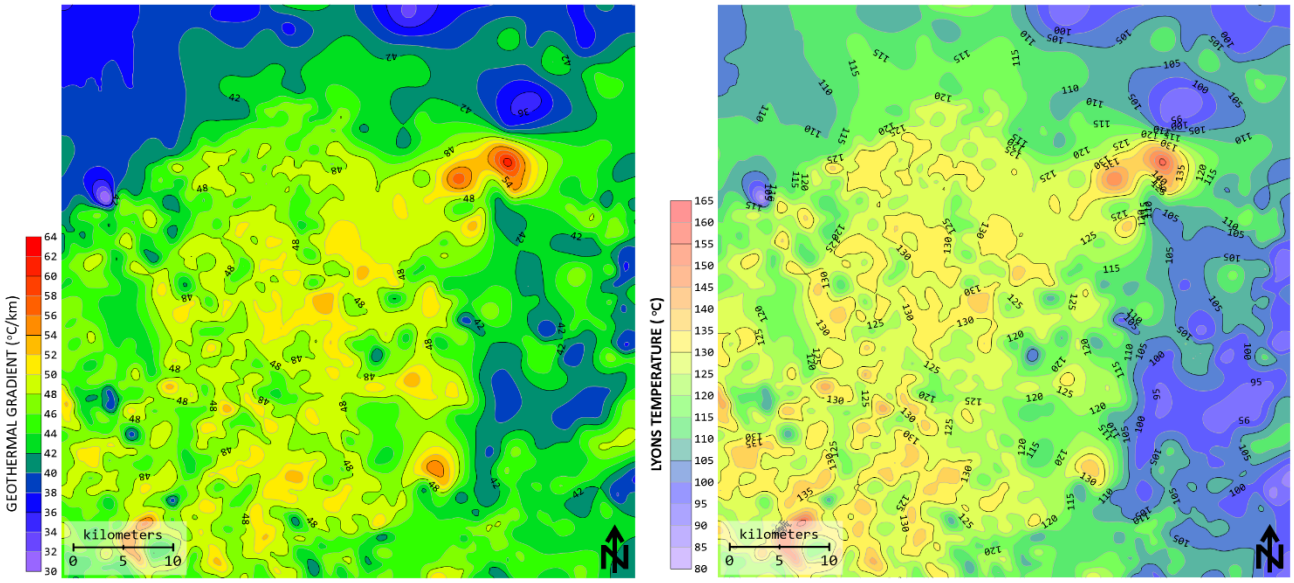

Figure 6: LEFT – Geothermal gradients in a portion of the Wattenberg "hot spot". RIGHT – Temperature at the top of the Lyons Fm.

Flow-capacity is analogous to phi*h but instead evaluates permeability. Flow-capacity is computed by using the horizontal porosity-permeability transform (Figure 4) to convert the density-porosity logs into permeability logs. Then each permeability value is multiplied by the sampling interval and the results are summed for the entire formation. Figure 7, right, was computed using only permeabilities ≥40mD.

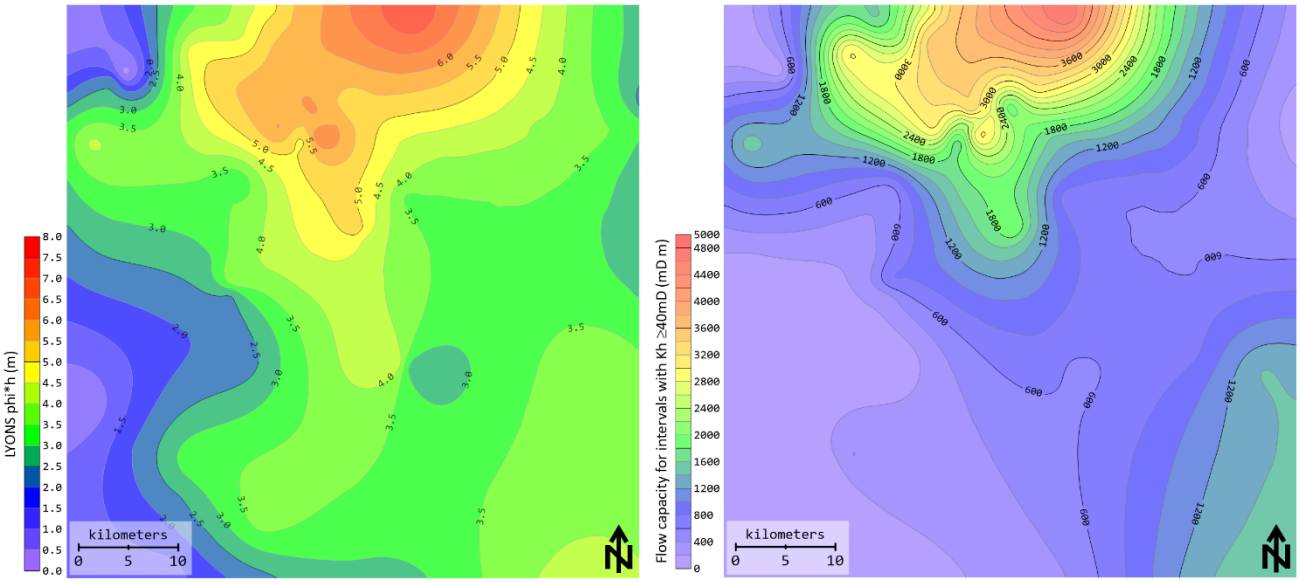

Figure 7: Maps of the Lyons Fm. in the study area from well data. LEFT – phi*h map. RIGHT – Flow-capacity (Kh*h) map.

3.3 Heat content

To compute the amount of heat in the formation, we need estimates of the heat capacity of brine and rock.

The brine salinity (120,000 ppm NaCl equivalent) was determined from brine samples and resistivity logs. The pressure at the top of the Lyons was estimated from oilfield pressure data and the depth to the top of the Lyons. The brine temperature was estimated using the temperature map of the top of the Lyons. Using the map grids of these values and an equation of state, we calculated a map of the heat capacity of the brine, which was found to vary by only about 3% in the study area (3.78-3.91 kJ/kg °C) Figure 8, left).

The heat capacity of the rock was estimated as follows: Waples and Waples (2004) give the following values for a sandstone at 20°C

- Density = 2.64 g/cm^3 = 2,640 kg/m^3
- Cp = specific heat capacity = 775 J/kg/K
- Cv = volumetric heat capacity = 2.05 J/cm^3/K = 2.05 MJ m^{-3} K^{-1}

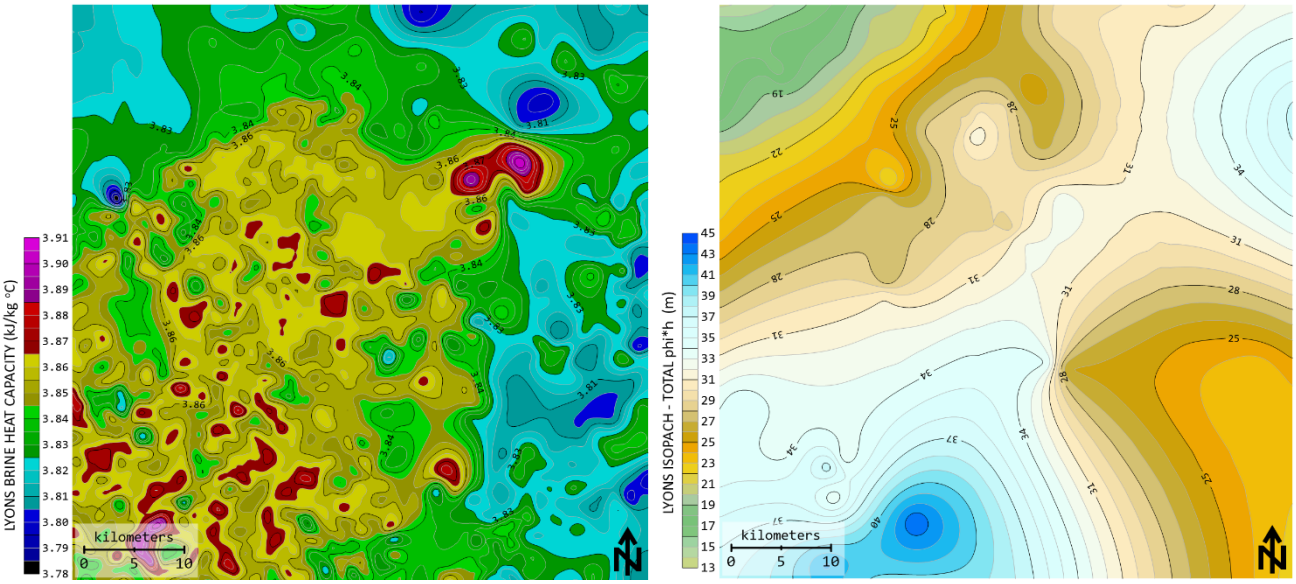

Figure 8: Maps of the study area. LEFT – Heat capacity of the Lyons brine. RIGHT – Thickness of the solid fraction of the Lyons.

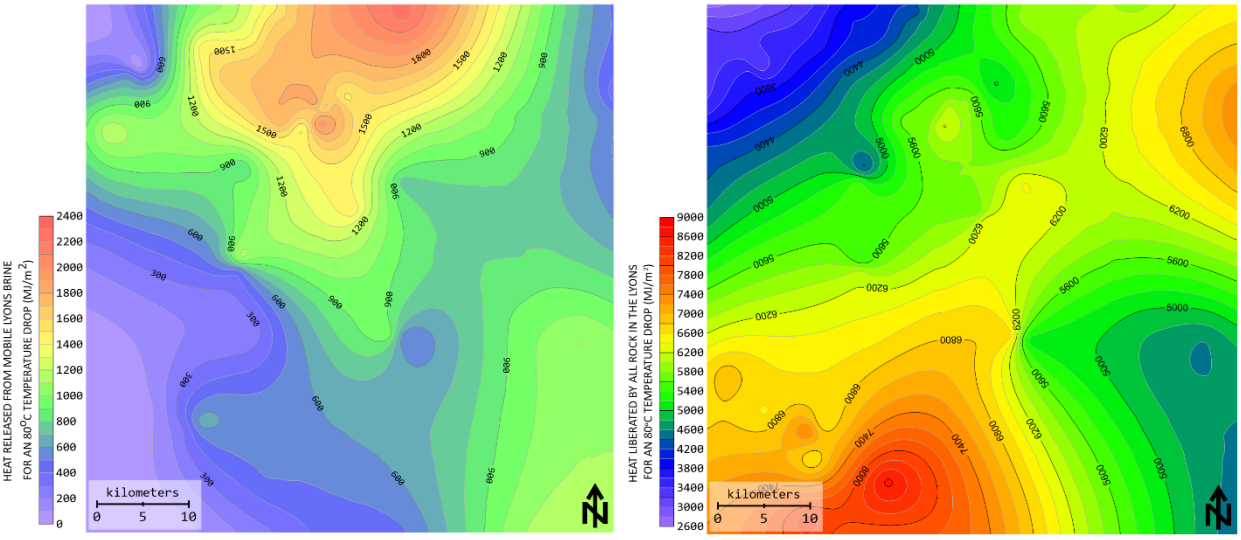

Figure 9: Maps of the study area showing the heat released for an 80°C temperature drop per square meter of formation. LEFT – Heat released from Lyons brine in the effective porosity (≥10%). RIGHT – Heat released from the solid fraction of the Lyons.

Equations 18 and 19 of Waples and Waples (2004) provide a method to estimate the heat capacity of a rock at a temperature different from the temperature at which the heat capacity was measured. Using this method yields C_p of the sandstone for the temperature range expected in the prospective area (2.46-2.47 MJ m^{-3} K^{-1}). We can use these as C_v values using the density measured at 20°C because the thermal expansion of sandstone is negligible compared to the uncertainties of our data (Somerton, 1992). Subtracting the phi*h map

grid from the Lyons isopach map grid produces a map of the thickness of the solid part of the Lyons, as if all the porosity was crushed out of the rock so that only the solid remains (Figure 8, right).

Using the phi*h map grid, the Lyons temperature map grid, and the brine heat capacity we can compute the heat content of the brine and rock as follows: The heat in a substance is given by: $Q = \text{mass } C_p \Delta T$. Mass is given by the density of the brine in kg/m^3 multiplied by the phi*h map grid. Using this formula gives the mass of brine in a 1 m^2 cylinder of brine of height phi*h. C_p is provided by the Cp map grid of the brine, or the values given above for the rock. The value of ΔT is given by the estimated temperature drop in the Organic Rankine Cycle (ORC) generating system on the surface, which is 80°C. Using these values for the brine in the effective porosity and the solid fraction of the Lyons produces the maps in Figure 9.

Exploiting an HSA requires withdrawing water, converting some of the heat to electricity in an ORC, then reinjecting the now cool water back into the formation both to dispose of the water and to maintain the reservoir pressure. Injected water gains heat as it flows through the rock eventually reaching the producing well. Eventually, the temperature of the produced water drops to a temperature that is uneconomic. The heat available for producing electricity is therefore the heat in the mobile brine, a fraction of the heat in the solid rock, and a fraction of the heat in the porosity fraction <10%.

3.4 Potentiometric surface and power maps

Producing electricity from an HSA requires getting the subsurface water to the ORC on the land surface. In an underpressured reservoir such as the Lyons, this requires pumping. The energy required for pumping represents a substantial parasitic load that is supplied by the electricity generated by the ORC, although this may be partially alleviated by injection well pressure support and thermosiphoning (e.g., Esmaeilpour et al., 2022), which effect is used presently by Eavor-Lite solely as their pumping system in a closed-loop installation (Zatonski and Brown, 2023). The depth of the potentiometric surface below the ground is therefore an important parameter for determining the economic viability of a prospect.

A map of the depth of the potentiometric surface is produced by subtracting the potentiometric surface depth from a digital elevation model of the terrain. Pumping power consumption is mapped using the map grid of the potentiometric surface depth and a function that describes required pumping power as a function of depth. ORC power production is mapped with the temperature map grid, the heat capacity map grid, and a function for ORC efficiency. With these latter two maps, the net power production can be mapped.

3.5 Identifying a prospect

Prospects were identified using the maps described in this section and additional maps (primarily variations on the maps presented here). Modeling the reservoir performance based on the mapped rock properties, the pumping costs, and other costs such as equipment, grid connection, and additional parasitic loads from the ORC identified desirable locations for power generation.

4. RESERVOIR SIMULATION

GTI has pursued two reservoir simulation efforts: Simple exploratory modeling with COMSOL (modeling by Johns Hopkins University) and geologically detailed modeling with FracMan (software and modeling by WSP, formerly Golder Associates; WSP, 2021). Cottrell et al (2023) provides a detailed discussion of the FracMan simulation effort. We briefly review it here. COMSOL models rely on uniform porosity and permeability (i.e. the average values) while the FracMan models use a detailed static model.

The detailed static model was built using density porosity logs from 16 representative wells in the area (Cottrell et al, 2023). The model captures the complex vertical and lateral variations of this eolian sandstone which is composed of dune sands and damp interdune deposits. Figure 10 is a vertical slice through the three-dimensional porosity model. The porosity model was converted to a permeability model using the horizontal porosity-permeability transform (Figure 4).

Figures 11, 12, and 13 compare the two modeling efforts. The flow fields (Figures 11 and 12) reflect the architecture of the models, namely, two parallel horizontal wells (production and injection) producing a dipole pressure field inducing a large flow field within the Lyons. The regular, symmetrical flow of the COMSOL model (Figure 11) results from the uniform porosity/permeability used in the simulation. In contrast, the complex structure of the detailed model (Figure 12) shows complex three-dimensional flow, although this result is broadly similar to the previous model. The temperature of the produced water over 20 years (Figure 13) shows little difference between the models despite the different starting temperatures, which reflects both the high porosity and permeability of the Lyons and the thickness of the Lyons (~40m) relative to the well spacing (600–800 m). For the same reasons, using anisotropic (vertical and horizontal) permeability (Figure 4) has little effect on the results. The unstable early time results of the COMSOL model reflect the long time-steps used for the simulation and the starting temperature of 20°C (Figure 11).

In the detailed model, minor short-cutting from the injector to the producer through high-permeability streaks leads to a slightly lower temperature at 20 years despite the greater distance between the wells. In both cases, the produced water temperature remains economical for generating electricity for over 20 years.

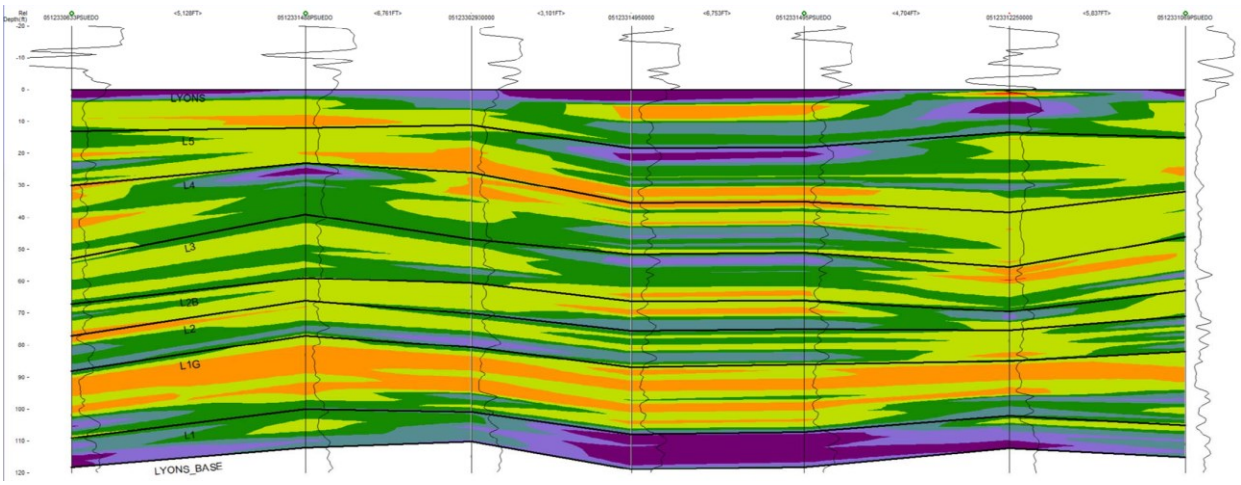

Figure 10: Vertical slice through the porosity model. The density-porosity logs used to make this slice of the model are shown. Porosity values were interpolated in 3D between the stratigraphic boundaries shown by the black lines. Higher porosity values are shown by warmer colors.

The produced water temperature is maintained for two reasons. Most importantly, the injected water gains heat from the rocks as it flows through the pore space. This contrasts with hydrothermal or Enhanced Geothermal System (EGS) geothermal in which the water is flowing through fractures in which the fracture surfaces cool progressively which can leave heat stranded because of the low thermal conductivity of rock. Flow through the pore space more completely extracts heat from the rock. An additional, lesser but vital, source of longevity is that the stimulated advective flow (Figures 11 and 12) increases the supply of virgin reservoir water to the production well. GTI's GenaSys™ system for geothermal heat harvesting incorporates these effects and proprietary GTI technologies.

These results demonstrate the viability of generating electricity from HSAs, even underpressured HSAs such as the Lyons in the DJ Basin. The detailed modeling shows the importance of the reservoir's porosity/permeability structure and hence the need to manage short-cutting. The detailed porosity/permeability structure cannot be determined prior to drilling so that any problematical short cutting must be managed with downhole flow controllers in both the injector and producer (Figure 14). Flow will be monitored with a fiber optic line with periodically spaced heaters (Figure 14). This monitoring system is proven in both oil and gas and groundwater projects (Briggs et al, 2016; Selker and Selker, 2018; Jin et al, 2019; Munn et al, 2020).

5. SUMMARY

This study provides a workflow for, and example of, exploration for, and simulation of, a Hot Sedimentary Aquifer geothermal prospect using the abundant data collected by the oil and gas industry. Such rich data sets are only available in oil and gas fields, which tend to be hotter than surrounding areas and hence are desirable targets for geothermal exploration. HSA geothermal electricity production will greatly expand the geographic coverage of geothermal electricity generation.

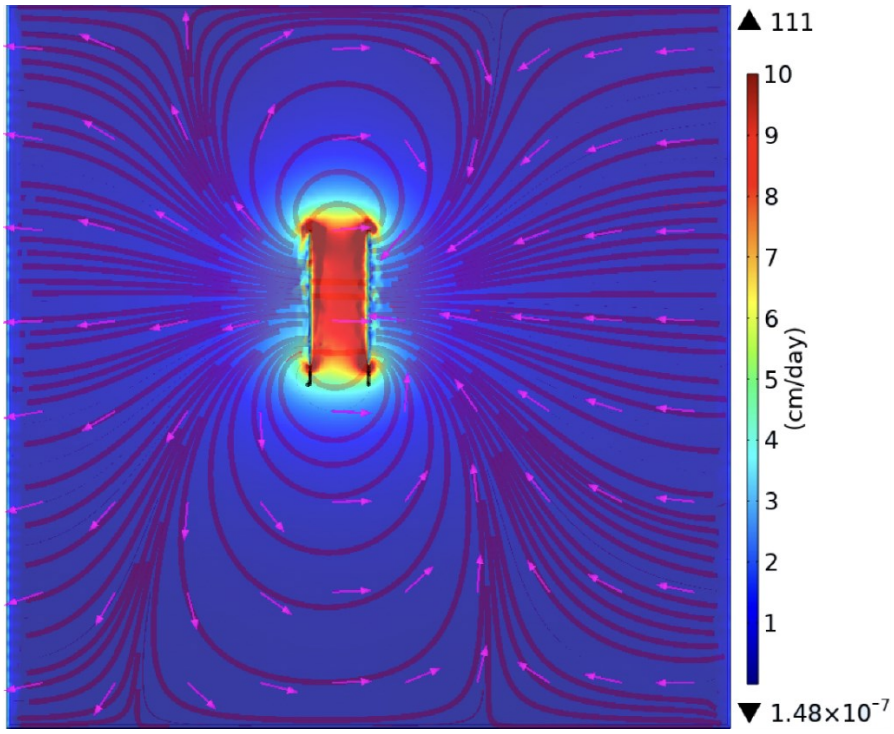

Figure 11: Horizontal slice of a COMSOL reservoir model at the depth of the production and injection wells after 20 years of production. Colors show fluid flow velocity in cm/day. Arrows show flow direction. 600m well spacing.

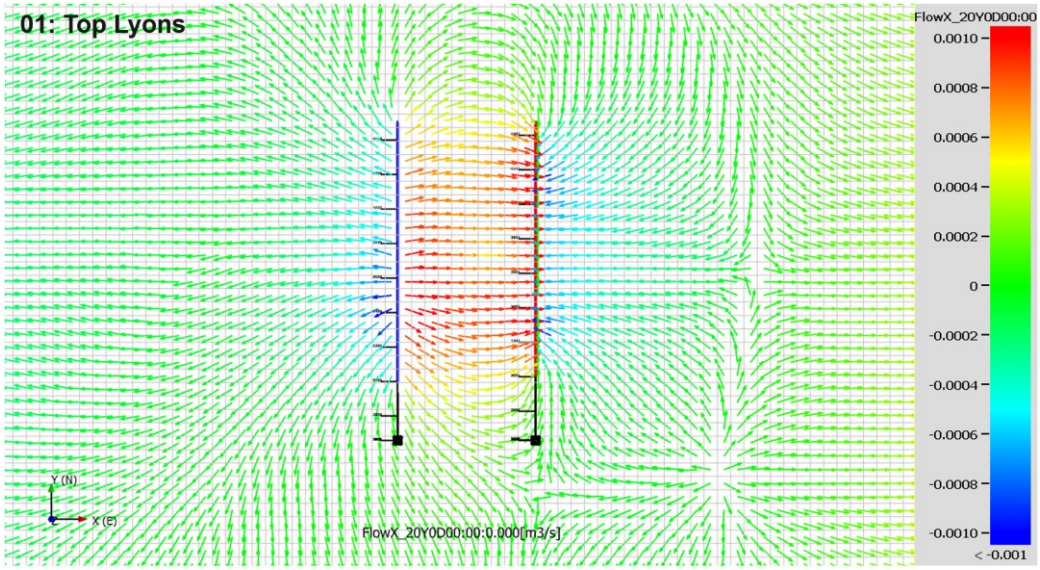

Figure 12: Horizontal slice of a FracMan reservoir model at the depth of the production and injection wells after 20 years of production. Colors show fluid flow velocity in m^3/s. Arrows show flow directions. The complex patterns reflect the complexity of the 3D porosity/permeability model. 800m well spacing.

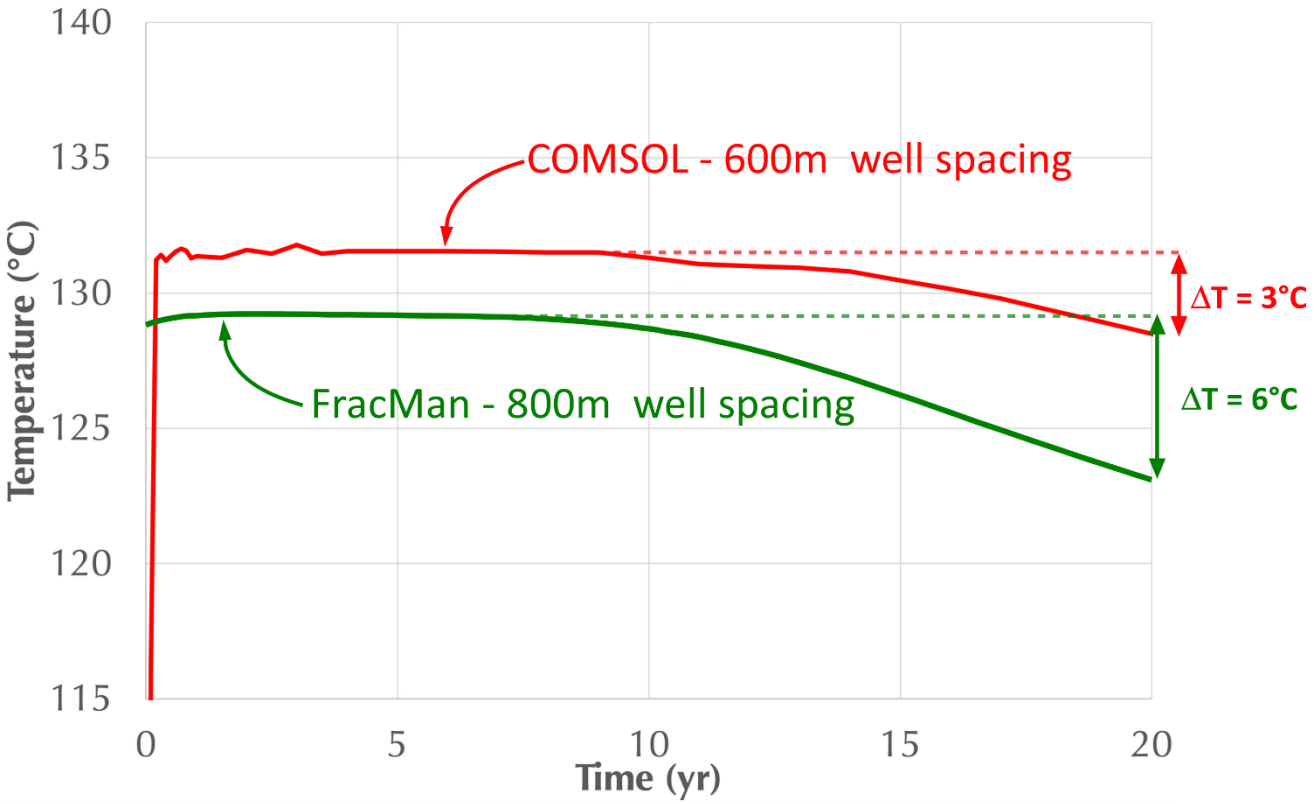

Figure 13: Produced water temperature over 20 years. The two models have different starting tempeartures. Although the temperature declines slightly it remains adequate for commercial electricity generation in both cases.

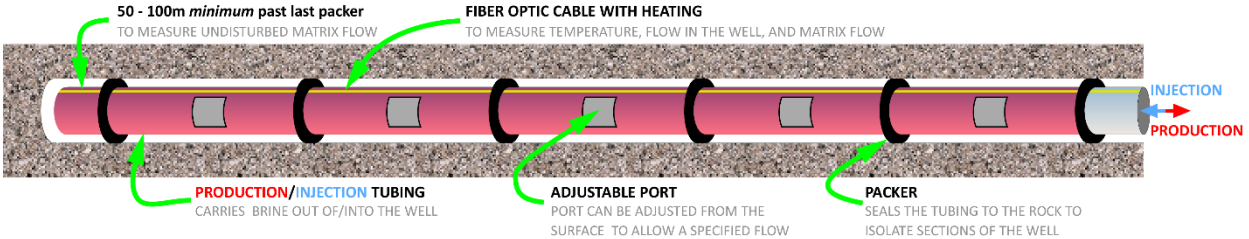

Figure 14: Schematic diagram (not to scale) showing how production and injection wells will be completed. Tubing centralizers are not shown. The well is not cased.

ACKNOWLEDGEMENTS

We thank and acknowledge White Eagle Exploration and Chevron for sharing data, the staff of the Colorado Energy and Carbon Management Commission (formerly named the Colorado Oil and Gas Conservation Commission) for helping resolve access problems to publicly available data, and the staff of the Denver U.S.G.S. for access to their cores and thin sections. We thank GTI and WSP for permission to publish. The interpretations presented here are entirely our own.

REFERENCES

Briggs, Martin A., Sean F. Buckley, Amvrossios C., Bagtzoglou, Dale D., Werkema, John W. Lane Jr.: Actively heated high-resolution fiber-optic-distributed temperature sensing to quantify streambed flow dynamics in zones of strong groundwater upwelling: Water Resources Research 52 (7), (2016) 5179–94.

Corrigan, J. and Bergman, S.: Thermal modeling and interpretation of thermal indicator data, AAPG Convention and Exhibition, San Diego, CA (1996).

Corrigan, J.: ZetaWare utilities – BHT correction homepage, correcting bottom hole temperature data, ZetaWare, Inc, http://www.zetaware.com/utilities/bht/default.html (2003, accessed 2021).

Cotrell, M., Lacazette, A., Chmela, B., Karimi, S., Marsh, B.D.: Evaluating the geothermal potential of hot sedimentary aquifers using a hybrid approach, 57th US Rock Mechanics/Geomechanics Symposium, ARMA 23-0422 (2023).

Esmaeilpour, M., Korzani, M. G., Kohl, T., Impact of thermosiphoning on long-term behavior of closed-loop deep geothermal systems for sustainable energy exploitation. Renewable Energy 194 (2022) 1247-1260.

Jin, Ge, Kyle Friehauf, Baishali Roy, Jesse J. Constantine, Herbert W. Swan, Kyle R. Krueger, and Kevin T. Raterman: Fiber optic sensing-based production logging methods for low-rate oil producers: In Proceedings of the 7th Unconventional Resources Technology Conference, 1183–99. Tulsa, OK, USA: Unconventional Resources Technology Conference (URTeC); Society of Petroleum Engineers (2019).

Kendigelen, O., Egenhoff, S., Matthews, W.A., Holm-Denoma, C.S., Whiteley, K.R., Gent, V.A., Longman, M.W., Hagadorn, J.W., The edge of a Permian erg: Eolian facies and provenance of the Lyons Sandstone in northern Colorado: Rocky Mountain Geology, v. 58, no. 2, (2023) 57-82, doi:10.24872/rmgjournal.58.2.57.

Lee, M.-K., Bethke, C.M.: Groundwater flow, late cementation, and petroleum accumulation in the Permian Lyons Sandstone, Denver Basin, AAPG Bull, 78, (1994) 221-241.

Levandowski, D.W.; Kaley, M.E.: Silverman, R.; Smalley, R.G.: Cementation in Lyons Sandstone and its role in oil accumulation, Denver Basin, Colorado, AAPG Bull, 57 (1973) 2217-2244.

Longman, M.: Petrographic study of the Lyons Sandstone in the Wattenberg Field area: Assessment of its geothermal reservoir potential (2021), Geothermal Technologies, Inc. proprietary study.

Munn, J. D., C. H. Maldaner, T. I. Coleman, and B. L. Parker. 2020. Measuring fracture flow changes in a bedrock aquifer due to open hole and pumped conditions using active distributed temperature sensing, Water Resources Research 56 (10) (2020) 1–23.

Nelson, P.H., Gianoutsos, N.J., Drake, R.M. III: Underpressure in Mesozoic and Paleozoic rock units in the Midcontinent of the United States, AAPG Bull, 99 (2015) 1861-1892.

Selker, Frank, and John S. Selker: Investigating water movement within and near wells using active point heating and fiber optic distributed temperature Sensing, Sensors 18 (4) (2018) https://doi.org/10.3390/s18041023.

Somerton, W.H. *editor*: Thermal properties and temperature-related behavior of rock-fluid systems, Chapter IV – Thermal expansion of rocks: Developments in Petroleum Science, Elsevier (1992) ISBN 0-444-89001-7

Waples, D.W. and Waples, J.S.: A Review and Evaluation of Specific Heat Capacities of Rocks, Minerals, and Subsurface Fluids. Part 1: Minerals and Nonporous Rocks: Natural Resources Research, Vol. 13, No. 2, (2004) p. 97-122.

White, M., Vasyliv, Y., Beckers, K., Martinez, M., Balestra, P., Parisi, C., Augustine, C., Bran-Anleu, G., Horne, R., Pauley, L., Bettin, G., Marshall, T., Bernat, A.: Numerical investigation of closed-loop geothermal systems in deep geothermal reservoirs. Geothermics, 116, 102852 (2024) p.1-18.

WSP UK Ltd., FracMan 8.1 Energy Edition software (2021).

Zatonski, V., Brown, C.: Eavor-Lite Update After Four Years of Operation. GRC Transactions, Vol. 47, (2023), p. 1-9.

Zhou, M., Optimization of well configuration for a sedimentary enhanced geothermal reservoir, M.S. Thesis, Colorado School of Mines (2016), 86 p.

Zhou, M., Cho, J., Zerpa, L.E., Augustine, C., Optimization of well configuration for a sedimentary enhanced geothermal reservoir, GRC Transactions, v. 40 (2016) 14 p.